

# On the Effectiveness of Random Weights in Graph Neural Networks

Thu Bui<sup>1</sup>, Carola-Bibiane Schönlieb<sup>2</sup>, Bruno Ribeiro<sup>1</sup>, Beatrice Bevilacqua<sup>1</sup>, Moshe Eliasof<sup>2</sup>

<sup>1</sup>Department of Computer Science, Purdue University, West Lafayette, IN, USA

<sup>2</sup>Department of Applied Mathematics, University of Cambridge, Cambridge, UK

## Abstract

Graph Neural Networks (GNNs) have achieved remarkable success across diverse tasks on graph-structured data, primarily through the use of learned weights in message passing layers. In this paper, we demonstrate that random weights can be surprisingly effective, achieving performance comparable to end-to-end training counterparts, across various tasks and datasets. Specifically, we show that by replacing learnable weights with random weights, GNNs can retain strong predictive power, while significantly reducing training time by up to  $6\times$  and memory usage by up to  $3\times$ . Moreover, the random weights combined with our construction yield random graph propagation operators, which we show to reduce the problem of feature rank collapse in GNNs. These understandings and empirical results highlight random weights as a lightweight and efficient alternative, offering a compelling perspective on the design and training of GNN architectures.

## 1 Introduction

Graph Neural Networks (GNNs) have emerged as a powerful tool for modeling and analyzing graph data Bronstein *et al.* [2021]. Traditionally, GNNs rely on learnable weights in their message-passing layers, which are optimized through end-to-end training to extract meaningful representations from graph data. While this paradigm has led to consistency performance, it also raises an intriguing question: *Are learned weights always necessary for effective message passing?*

Previous studies have explored the role of randomization in neural network architectures. Random weights have been successfully applied in models like Extreme Learning Machines (ELMs) [Zhang *et al.*, 2020, 2023] and Random Reservoir-Computing GNNs [Gallicchio and Micheli, 2020; Pasa *et al.*, 2021; Huang *et al.*, 2022a; Navarin *et al.*, 2023], demonstrating that random and fixed projections can capture meaningful representations without extensive training. Specifically, they rely on a random fixed set of weights, followed by a solution of a dynamic system based on these random weights. However, these approaches often lack a sys-

tematic understanding of why and how random weights contribute to effective learning.

In this paper, *we investigate the effectiveness of using random weights in GNNs as a replacement for learned parameters in message-passing layers.* Surprisingly, we find that GNNs with random weights can achieve performance comparable to their fully trained counterparts across a variety of graph tasks and datasets. This observation challenges the conventional reliance on end-to-end training to achieve strong predictive power in GNNs.

To leverage the benefits of randomization, we propose **Random Propagation GNN (RAP-GNN)**. Our method employs diagonal weight matrices, sampled on-the-fly at each forward pass, in combination with a simple pretrained node embedding layer. The diagonal structure preserves essential information about the dynamics of message passing while significantly reducing the number of parameters at each layer.

Beyond their effectiveness in terms of downstream performance, we show that random weights also offer computational advantages. By eliminating the need for gradient-based optimization of message-passing weights, RAP-GNN reduces training time by up to  $6\times$  and memory consumption by up to  $3\times$ . Moreover, we provide insights into why random weights are effective, by interpreting them as random graph propagation operators, which, combined with the diagonal weight structure, help to mitigate common GNN issues such as feature collapse during message passing.

Our findings suggest that random weights are not merely a computational shortcut but a principled design choice for scalable and effective GNN architectures, opening up new possibilities for resource-efficient graph learning systems.

The paper is organized as follows: In Section 2, we review works related to our approach. Section 3 introduces RAP-GNN, highlighting its design and key advantages. We begin by outlining the architecture in Section 3.1, followed by an exploration of the critical issue of feature collapse in Section 3.2—a phenomenon where node embeddings lose diversity across layers. Next, in Section 3.3, we discuss the symmetry-preserving capabilities of RAP-GNN, showcasing its flexibility to function as either a permutation-sensitive or permutation-equivariant GNN, making it adaptable to a wide range of applications. Finally, in Section 4, we report an extensive set of experiments to demonstrate the effectiveness of RAP-GNN.

## 2 Related Work

The idea of using random weights as a substitute for learned parameters has been explored in various neural network paradigms. In the following, we discuss these approaches and provide additional references in Appendix B.

**Random Reservoir Computing (RC).** Reservoir Computing (RC) is a computational framework introduced by Jaeger [2001], which leverages fixed, randomly sampled weights to parameterize a high-dimensional reservoir, i.e., a recurrent network that processes input data and projects it into a richer feature space. Traditional, i.e., non-neural, RC methods typically rely on recurrent forward passes until convergence or a predetermined number of iterations, and were shown to benefit graph tasks [Gallicchio and Micheli, 2010]. Later, FDGNN [Gallicchio and Micheli, 2020] extended RC principles to GNNs for graph classification, where stability constraints are met in a recurrent setting. MRGNN [Pasa *et al.*, 2021] built on this by “unrolling” the recurrent layer, reducing time complexity while maintaining the benefits of reservoir dynamics. Despite these advancements, RC-based methods maintain fixed random weights, sampled only once at the beginning of training and used throughout. In contrast, our RAP-GNN advocates for sampling new weights at each iteration. Moreover, RC methods are designed with specific architectures and graph tasks in mind (primarily for graph classification) whereas our RAP-GNN represents a general framework that can be coupled with any GNN architecture to solve any graph task, enhancing its adaptability across various graph learning tasks.

**Extreme Learning Machines (ELM).** Another area of research has explored ELMs [Huang *et al.*, 2006], which have recently been adapted for graph learning [Zhang *et al.*, 2020; Gonçalves and Nonato, 2022; Zhang *et al.*, 2023]. ELMs enable efficient training by using analytic, non-iterative learning techniques. However, in graph learning, these methods were shown to be constrained to two GNN layers and assume that the weights in the hidden layer are *random and fixed* throughout the training process. This constraint hinders the ability of ELMs to leverage deep networks, which can be important for capturing the complex behaviors in the data. In contrast, as shown in our experiments, our RAP-GNN is effective across a variable number of layers and ensures that random weights are sampled at every forward pass, leading to more propagations seen during training time, and overall improved downstream performance. Additionally, by constraining RAP-GNN to use *fixed full* (i.e., *non diagonal*) *random weights*, a variant we denote as Fixed Random Weights in our experiments, our approach can implement ELM. Thus, RAP-GNN can also be considered as a generalization of ELMs.

**Random Node Features (RNF).** Besides random graph models in terms of their weights, another research line suggests sampling random node features (RNF) to obtain theoretically improved performance [Murphy *et al.*, 2019; Abboud *et al.*, 2021; Sato *et al.*, 2021; Puny *et al.*, 2020]. In addition, the propagation of RNF has proven effective as a positional encoding technique [Eliasof *et al.*, 2023a] or within the normalization layer [Eliasof *et al.*, 2024]. Differently, RAP-

GNN studies the value of random weights within the model, not random input features.

## 3 Method

This section introduces our RAP-GNN, a novel approach that utilizes diagonal random weights in the message passing layers of GNNs. In RAP-GNN, the weights in each GNN layer are diagonal matrices, randomly sampled from a uniform distribution during each forward pass, thus eliminating the need for learning them.

We begin by detailing the architectural components in Section 3.1, providing an overview in Figure 1 and pseudocode in Appendix A. In Section 3.2, we introduce the concept of feature collapse, a significant challenge in GNNs, where node embeddings lose diversity and converge to nearly identical values as the number of layers increases. We demonstrate that RAP-GNN effectively addresses this issue, ensuring stability even in deeper architectures. Finally, in Section 3.3, we discuss the symmetry-preserving properties of RAP-GNN, showing how it can be either permutation-sensitive or permutation-equivariant.

**Notations.** In this paper we denote a graph by the tuple  $G = (V, E)$ , where  $V$  is the set of  $n$  nodes and  $E$  is the set of  $m$  edges. We further denote by  $\mathbf{A} \in \{0, 1\}^{n \times n}$  the adjacency matrix of the graph. We assume that the nodes are equipped with input node features of dimensionality  $c$ , denoted by  $\mathbf{x} \in \mathbb{R}^{n \times c}$ , and denote by  $\mathbf{x}_i$  the  $i$ -th row of  $\mathbf{x}$ , which contains the features for node  $i$ . Throughout this paper, we will consider GNNs and denote the number of layers as  $L$ .

### 3.1 RAP-GNN

Our RAP-GNN consists of three key components: (i) a node embedding layer  $f_\phi^{\text{pre}}$ , which is applied point-wise to the input node features of each node to obtain initial node embeddings  $\mathbf{h}^{(0)} = f_\phi^{\text{pre}}(\mathbf{x})$ , (ii) a stack of  $L$  GNN layers interleaved with non-linearities, where each layer  $l = 1, \dots, L$  is denoted by  $g_{\mathbf{w}^{(l)}}$  and consists of one GNN layer with parameters  $\mathbf{w}^{(l)}$  followed by a non-linear activation function, returning node embeddings, that is  $\mathbf{h}^{(l)} = g_{\mathbf{w}^{(l)}}(\mathbf{h}^{(l-1)}, \mathbf{A})$ , and (iii) a classifier  $c_\theta$ , that takes the node embeddings and return a final prediction. The embedding layer  $f_\phi^{\text{pre}} : \mathbb{R}^c \rightarrow \mathbb{R}^d$  maps the  $c$  input features into a hidden-dimensional space  $d$ , and is a multi-layer perceptron (MLP) or a single GNN layer. Each layer  $g_{\mathbf{w}^{(l)}} : \mathbb{R}^{n \times d} \times \mathbb{R}^{n \times n} \rightarrow \mathbb{R}^{n \times d}$  processes these embeddings along with the adjacency matrix, with weights  $\mathbf{w}^{(l)}$ ,  $l \in \{1, \dots, L\}$ . In our RAP-GNN, each  $\mathbf{w}^{(l)} \in \mathbb{R}^{d \times d}$  is a diagonal matrix, where the diagonal values are randomly and uniformly sampled at each forward pass. This randomness eliminates the need to learn the GNN layer weights. If  $f_\phi^{\text{pre}}$  were learnable, backpropagation would still be required, even though the GNN layer weights would not be updated. However, we avoid this by pretraining  $f_\phi^{\text{pre}}$  separately, ensuring there is no backpropagation through the GNN. Finally, the classifier  $c_\theta : \mathbb{R}^d \rightarrow \mathbb{R}^o$  maps the processed representations (node or graph depending on the task) to the target output dimension  $o$  to obtain the final prediction  $\hat{y} = c_\theta(\mathbf{h}^{(L)})$ ,

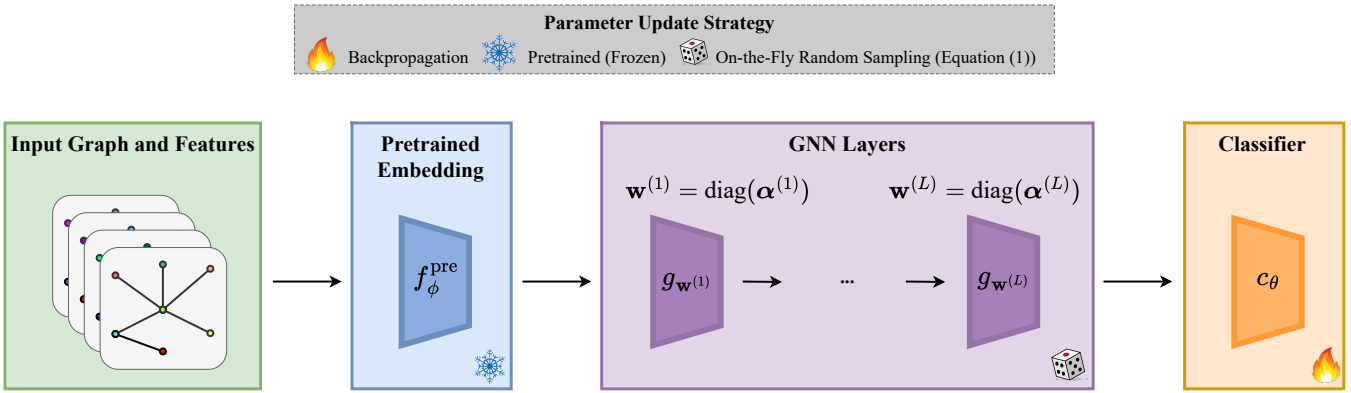


Figure 1: Illustration of RAP-GNN. The pretrained embedding  $f_\phi^{\text{pre}}$  is frozen, while the classifier  $c_\theta$  is optimized. All GNN weights,  $\mathbf{w}^{(l)}$ ,  $l = 1, \dots, L$  are diagonal matrices, randomly sampled on-the-fly in each forward pass.

with only the classifier parameters  $\theta$  being trained during the learning process. The model is trained in two phases:

**(i) Pretraining Phase.** In RAP-GNN,  $f_\phi^{\text{pre}}$  is responsible for processing input node features and mapping them into the desired hidden dimension  $d$ . Importantly,  $f_\phi^{\text{pre}}$  is trained in a pretraining phase to generate meaningful input representations. This pretraining step eliminates the need to train  $f_\phi^{\text{pre}}$  end-to-end during the main training phase, which would otherwise require backpropagation through the randomly sampled weights in the GNN layers.

The embedding layer  $f_\phi^{\text{pre}}$  is pretrained using a simple MLP or a single GNN layer,  $f_\phi^{\text{pre}} = c_{\phi'}^{\text{pre}} \circ f_{\phi'}^{\text{pre}}$ , optimizing the downstream task. Once the embedding layer has been pretrained, we use  $\phi$  during the main training phase, while keeping it frozen, allowing the model to learn only the classifier on the network.

**(ii) Training Phase.** In the training phase, the key innovation is the introduction of randomness in GNN layers. Namely, during each forward pass, a new random diagonal weight matrix  $\mathbf{w}^{(l)}$  is sampled for each GNN layer  $l$  as follows:

$$\mathbf{w}^{(l)} = \text{diag}(\boldsymbol{\alpha}^{(l)}), \quad (1)$$

where  $\boldsymbol{\alpha}^{(l)} = [\alpha_1^{(l)}, \dots, \alpha_d^{(l)}]$  is a vector randomly sampled from a uniform distribution, with  $d$  being the hidden dimension, and  $l = 1, \dots, L$ , with  $L$  the total number of GNN layers in the network. *Our motivation* for choosing the diagonal structure in Equation (1) over a full random matrix is three-fold: (i) using a diagonal matrix for  $\mathbf{w}^{(l)}$  replaces matrix multiplication with element-wise vector multiplication, reducing resource-intensive operations and accelerating both training and inference time, as demonstrated later in Section 4.3; (ii) ensures that each feature is propagated independently by the corresponding  $\alpha_i^{(l)}$ , preventing random weights from overly mixing the features; and (iii) mitigates feature rank collapse, as demonstrated in Observation 2. By constraining the values of  $\mathbf{w}^{(l)}$  to the interval  $[0, 1]$  and using them as the weights of GNN layers such as GCN [Kipf and Welling, 2016], we achieve diffusion-like propagation, similar to Eliasof *et al.*

[2023b], which, in our case, because of the weights sampling approach, yields random graph propagation operators.

Note that, in this training phase, only the parameters  $\theta$  of the classifier  $c_\theta$  are to be learned based on the loss function, while  $\mathbf{w}^{(1)}, \dots, \mathbf{w}^{(L)}$  and  $\phi$  are not learned. This eliminates the need for backpropagation through the GNN layers, significantly reducing computational costs, as illustrated in Figure 2, and discussed in Section 4.

**(iii) Inference with RAP-GNN.** During inference, the input is processed as a forward pass in the training phase, with random weights sampled from the uniform distribution.

## 3.2 Reducing Feature Collapse with RAP-GNN

Feature collapse is a critical issue in GNNs [Roth and Liebig, 2024], where node embeddings lose diversity and become nearly identical as the number of layers increases. This phenomenon hinders the ability of the network to learn and extract a variety of features to address downstream tasks, resulting in degraded performance. In this section, we consider feature collapse through the lens of feature matrix rank, defined below. Then, we theoretically demonstrate the impact of diagonal and full random matrices on node features rank, motivating the design choices in our RAP-GNN. Lastly, we supplement our theoretical understanding with empirical evidence discussed below.

Formally, let  $\mathbf{h}^{(l)} \in \mathbb{R}^{n \times d}$  denote the node embeddings at layer  $l$  of a GNN. We define the rank of  $\mathbf{h}^{(l)}$  as follows:

**Definition 1** (Node Embedding Rank). *Assuming  $n > d$ , the maximal rank of the node embedding matrix  $\mathbf{h}^{(l)}$  is  $d$ . Without loss of generality, let us denote the rank of  $\mathbf{h}^{(l)}$  as  $\text{rank}(\mathbf{h}^{(l)}) = d'$ , where  $1 \leq d' \leq d$ .*

The rank of the embedding matrix is a useful indicator of the diversity of node embeddings. A higher rank suggests more diverse embeddings, whereas a lower rank indicates feature collapse, because more features are linearly dependent. To better understand this phenomenon, we analyze the rank dynamics under two types of random weight matrices: (i) full random matrices, and (ii) diagonal random matrices, which we use in our RAP-GNN.

Specifically, we make the following observations, that highlight how the weight matrix structure affects the rank of the updated feature matrix, and why RAP-GNN effectively mitigates feature collapse.

**Observation 1** (Rank Collapse with Full Matrix). *Consider a full (i.e., non diagonal) matrix  $\mathbf{w}^{(l)} \in \mathbb{R}^{d \times d}$  whose entries are uniformly sampled between 0 and 1. Because in expectation, the value of each entry is 0.5,  $\mathbb{E}[\mathbf{w}^{(l)}]$  can be expressed as:*

$$\mathbb{E}[\mathbf{w}^{(l)}] = 0.5 \cdot \mathbf{1}_{d \times d},$$

where  $\mathbf{1}_{d \times d}$  is a  $d \times d$  matrix of ones. For simplicity, consider the update rule consisting only of the channel mixing operation defined as:

$$\tilde{\mathbf{h}}^{(l)} = \mathbf{h}^{(l)} \mathbf{w}^{(l)}.$$

In this case, we have:

$$\mathbb{E}[\tilde{\mathbf{h}}^{(l)}] = \mathbb{E}[\mathbf{h}^{(l)} \mathbf{w}^{(l)}] = \mathbf{h}^{(l)} \mathbb{E}[\mathbf{w}^{(l)}] = \mathbf{h}^{(l)} (0.5 \cdot \mathbf{1}_{d \times d}).$$

This implies that in expectation, each channel in  $\tilde{\mathbf{h}}^{(l)}$  will be a linear combination of the channels in  $\mathbf{h}^{(l)}$ , with the same coefficient of 0.5. Consequently, all columns in  $\tilde{\mathbf{h}}^{(l)}$  will be linearly dependent, resulting in  $\mathbb{E}[\text{rank}(\tilde{\mathbf{h}}^{(l)})] = 1$ .

Observation 1 demonstrates that using full random matrices can cause a significant reduction in rank, leading to rapid feature collapse as layers are stacked. In contrast, diagonal random matrices provide a more robust mechanism for preserving rank, as described next.

**Observation 2** (Rank Preservation with Diagonal Matrix in RAP-GNN). *Consider the case of diagonal random matrices  $\mathbf{w}^{(l)}$ , where the diagonal entries are uniformly sampled between 0 and 1. In expectation, each diagonal entry of  $\mathbf{w}^{(l)}$  has a value of 0.5. Thus,  $\mathbb{E}[\mathbf{w}^{(l)}]$  can be expressed as:*

$$\mathbb{E}[\mathbf{w}^{(l)}] = 0.5 \cdot \mathbf{I}_d,$$

where  $\mathbf{I}_d$  is the  $d \times d$  identity matrix. For simplicity, consider the update rule consisting only of the channel mixing operation defined as:

$$\tilde{\mathbf{h}}^{(l)} = \mathbf{h}^{(l)} \mathbf{w}^{(l)}.$$

In this case, each channel in  $\tilde{\mathbf{h}}^{(l)}$  is scaled independently by the corresponding diagonal entry. In expectation, each scaling factor is 0.5. Thus, the rank of  $\tilde{\mathbf{h}}$  remains unchanged, i.e.,

$$\mathbb{E}[\text{rank}(\tilde{\mathbf{h}})] = \mathbb{E}[\text{rank}(\mathbf{h}^{(l)})] = d'.$$

Observations 1 and 2 highlight the importance of the diagonal structure in random matrices used in RAP-GNN. By preserving the rank of the feature matrix across layers, RAP-GNN mitigates feature collapse and maintains diverse embeddings.

The observations above establish that RAP-GNN mitigates feature collapse especially when compared to GNNs with full random weights. In addition, we also observe in

Figure 4 that *in practice* RAP-GNN exhibits higher node embedding rank, and therefore less prone to feature collapse than end-to-end trained GNNs. Furthermore, we note that, although in principle, learnable weight matrices could adapt during training to mimic the behavior of RAP-GNN (e.g., becoming approximately diagonal and bounded), we empirically show in Figure 5 that the weight matrices in end-to-end trained GNNs do not approximate a diagonal structure after training.

### 3.3 On the Symmetry Preservation in RAP-GNN

In RAP-GNN, each weight matrix  $\mathbf{w}^{(l)}$  is sampled anew for every forward pass. This design ensures that the weights are consistent across all graphs within a batch but vary between batches. As a result, the output of RAP-GNN is permutation-equivariant for each individual graph, but not across different graphs. Specifically, isomorphic nodes within a graph receive identical representations, while isomorphic nodes across different graphs may have distinct representations due to differing weights used to obtain representations between the graphs.

This design positions RAP-GNN as a middle ground between permutation-equivariant GNNs, which consistently assign the same representation to isomorphic nodes regardless of their graph, and permutation-sensitive methods, such as those utilizing RNF, that differentiate all isomorphic nodes (with high probability). We believe that this hybrid approach facilitates more accurate predictions compared to RNF models, particularly in node classification tasks, as observed in our experiments. Since isomorphic nodes within a graph receive the same representation, the classifier does not need to map their distinct representations to the same prediction.

Notably, if we modify RAP-GNN by sampling new  $\mathbf{w}^{(l)}$  matrices only once per epoch, instead of for every forward call, the method becomes full permutation-equivariant within that epoch. With this modification, RAP-GNN consistently assigns the same representation to isomorphic nodes, regardless of their graph. Instead, if we incorporate RNF into RAP-GNN, it inherits the permutation-sensitive properties from RNF. With these alternative designs, RAP-GNN can act as a permutation-sensitive or permutation-equivariant GNN, or a hybrid of both. This flexibility enables users to tailor the model for various tasks that may require varying properties, broadening its applicability in different graph tasks.

## 4 Experiments

In this section we benchmark the performance of random weights in GNNs through our RAP-GNN, and compare it with various baselines and methods, on a variety of datasets and graph learning tasks. Below, we elaborate on these baselines, following by outlining the research questions that our experiments seek to address.

**Baselines.** To thoroughly evaluate the performance of RAP-GNN, we consider the following relevant baselines:

- (i) **Pretrained Embedding:** An embedding combined with a classifier is trained using an end-to-end method, intended for later use in RAP-GNN and the other baselines discussed below. A Pretrained Embedding can

Method ↓ / Dataset →	CORA	CITeseer	PUBMED
Pretrained Embedding	56.55 ± 0.7	54.35 ± 0.5	72.00 ± 0.4
End-to-End	81.50 ± 0.8	70.90 ± 0.7	79.00 ± 0.6
Fixed Random Diagonal	81.32 ± 0.8	70.12 ± 0.9	78.00 ± 0.9
Fixed Random Weights	58.70 ± 1.8	55.88 ± 1.2	71.52 ± 0.6
Random Weights	23.29 ± 9.2	45.85 ± 7.7	67.85 ± 1.7
RAP-GNN (Ours)	82.42 ± 0.3	70.75 ± 0.3	78.94 ± 0.4

Table 1: Node classification accuracy (%)↑ using a GCN backbone and different training strategies. RAP-GNN remains competitive or outperforms end-to-end training.

be either an MLP or a single-layer GNN, referred to as  $f_{\phi}^{\text{pre}}$  in the Pretrained phase illustrated in Figure 1. Additional details about the specific models used are provided in Appendix E.

- (ii) End-to-End: A GNN backbone with learnable weights, that is trained in an end-to-end fashion, as is standard when training neural networks.
- (iii) Fixed Random Diagonal: A variant using *fixed* random diagonal weight matrices  $\mathbf{w}^{(1)}, \dots, \mathbf{w}^{(L)}$  in Equation (1), that are sampled only once at network initialization, instead of sampling them on-the-fly.
- (iv) Fixed Random Weights: A variant using *fixed* random *full* matrices, that are sampled only once at network initialization, instead of sampling them on-the-fly. Notably, Fixed Random Weights follows a similar principle to ELMs, where the weight matrices are sampled once and held fixed.
- (v) Random Weights: A variant using random *full* matrices, that are sampled on-the-fly.

**Research Questions.** Our goal is to address the following key research questions:

- (Q1) How does RAP-GNN compare to end-to-end training and other baselines of GNN architectures in terms of downstream performance?
- (Q2) Is the choice of  $\mathbf{w}^{(l)}$ ,  $l = 1, \dots, L$  to be diagonal and sampled on-the-fly weight matrices superior to full or fixed random weights?
- (Q3) How efficient is our RAP-GNN compared with end-to-end training?

We present our main results below, with additional experimental findings in Appendix D. Particularly, Appendix D.1 demonstrates that alternative choices of random weight matrix structures underperform compared to our design of RAP-GNN, while Appendix D.2 underscores the significant role of embedding pretraining. Furthermore, RAP-GNN achieves accuracy comparable to end-to-end trained networks, while being significantly more efficient on large-scale datasets in Appendix D.3. We also show the robustness of RAP-GNN to varying batch sizes, confirming its practical adaptability, in Appendix D.4. Details on hyperparameter selection and dataset statistics are provided in Appendix E.

Method ↓ / Dataset →	MUTAG	PTC	PROTEINS
<b>RC METHODS</b>			
MRGNN	N/A	57.6 ± 10.0	75.8 ± 3.5
U-GCN	N/A	62.6 ± 1.4	74.1 ± 0.9
P-RGNN	N/A	N/A	71.1 ± 2.6
FDGNN	N/A	64.3 ± 5.4	76.8 ± 2.9
<b>BASELINES</b>			
Pretrained Embedding	85.7 ± 7.9	59.0 ± 4.5	73.2 ± 3.8
End-to-End	89.4 ± 5.6	64.6 ± 7.0	76.2 ± 2.8
Fixed Random Diagonal	88.4 ± 7.4	63.3 ± 7.8	74.3 ± 3.4
Fixed Random Weights	85.6 ± 7.8	62.8 ± 5.5	67.7 ± 5.0
Random Weights	74.0 ± 7.5	57.9 ± 8.4	60.3 ± 5.9
RAP-GNN (Ours)	90.4 ± 5.2	64.2 ± 9.8	75.9 ± 3.8

Table 2: Graph classification accuracy (%)↑ on TUDatasets. RAP-GNN is competitive to end-to-end training and outperforms Reservoir Computing (RC) methods.

#### 4.1 (A1) The Performance of RAP-GNN

We address Q1 by examining whether RAP-GNN, that performs on-the-fly diagonal weights sampling, can serve as an effective alternative to an end-to-end training approach in terms of performance. To evaluate this, we compare the performance of RAP-GNN against end-to-end trained networks and the aforementioned baselines across diverse graph tasks and datasets, leveraging various GNN backbones, detailed below.

**Planetoid Node Classification.** Table 1 presents the performance comparison on the node classification task using the Cora [McCallum *et al.*, 2000], CiteSeer [Sen *et al.*, 2008], and PubMed [Namata *et al.*, 2012] datasets. All experiments utilize a GCN backbone [Kipf and Welling, 2016] for the GNN layers with residual connections. The results demonstrate that RAP-GNN also outperforms the end-to-end baseline on the Cora dataset and remains competitive on CiteSeer and PubMed. Notably, the results also highlight the benefits of on-the-fly sampling of diagonal weights,  $\mathbf{w}^{(l)}$ , at each forward pass, because RAP-GNN outperforms all other baselines involving random weights—Fixed Random Diagonal, Fixed Random Weights, and Random Weights.

**TUDatasets Graph Classification.** Here, we evaluate RAP-GNN on a graph classification task. In our experiments, we use the popular GIN backbone [Xu *et al.*, 2019] on the TUDatasets [Morris *et al.*, 2020]. In addition to the baselines evaluated in Table 1, we include Reservoir Computing (RC) methods designed for graph classification and evaluated on the same datasets. The results in Table 2 demonstrate that RAP-GNN delivers competitive accuracy compared to end-to-end training. Furthermore, RAP-GNN, which employs randomly sampled diagonal weights on-the-fly, achieves accuracy comparable to Reservoir Computing methods such as MRGNN [Pasa *et al.*, 2021], U-GCN [Donghi *et al.*, 2024], P-RGNN [Bianchi *et al.*, 2022], and FDGNN [Gallicchio and Micheli, 2020], all of which rely on fixed random weights. These results underscore the effectiveness of RAP-GNN.

**Graph-level Tasks on OGB.** Additionally, we evaluate RAP-GNN on the OGB graph benchmark collection [Hu *et*

Method ↓ / Dataset →	MOLESOL RMSE ↓	MOLTOX21 ROC-AUC ↑	MOLHIV ROC-AUC ↑
Pretrained Embedding	1.235 ± 0.021	69.73 ± 0.39	70.97 ± 0.87
End-to-End	1.173 ± 0.057	74.91 ± 0.51	75.58 ± 1.40
Fixed Random Diagonal	1.114 ± 0.060	71.73 ± 0.48	74.74 ± 0.93
Fixed Random Weights	1.122 ± 0.014	67.54 ± 0.51	71.82 ± 1.28
Random Weights	1.148 ± 0.029	67.61 ± 0.32	71.61 ± 1.32
RAP-GNN (Ours)	1.083 ± 0.053	73.78 ± 0.51	76.04 ± 0.71

Table 3: Performance comparison of RAP-GNN on graph classification tasks. The results show that RAP-GNN achieves competitive performance to end-to-end trained GNNs. Additional results on the MOLBACE dataset are provided in Table 10.

Method ↓ / Dataset →	OGBN-PROTEINS ROC-AUC ↑	OGBN-PRODUCTS ACCURACY ↑
Pretrained Embedding	71.07 ± 0.36	72.83 ± 0.40
End-to-End	77.29 ± 0.46	75.90 ± 0.31
Fixed Random Diagonal	76.84 ± 0.32	74.93 ± 0.78
Fixed Random Weights	73.71 ± 0.71	27.72 ± 0.79
Random Weights	70.46 ± 0.74	26.08 ± 0.82
RAP-GNN (Ours)	77.01 ± 0.38	75.60 ± 0.88

Table 4: Classification performance on ogbn-proteins and ogbn-products using GCN [Kipf and Welling, 2016]. RAP-GNN is competitive to end-to-end training.

*et al.*, 2020] using the GINE backbone [Dwivedi *et al.*, 2023]. As shown in Table 3, RAP-GNN demonstrates superior performance on the ogbg-molhiv dataset and remains competitive on the ogbg-moltox21 dataset compared to end-to-end. Notably, RAP-GNN outperforms end-to-end on the regression task of the ogbg-molesol dataset, further highlighting its adaptability across various graph tasks. Results from the ogbg-molbace dataset, also part of the collection, are presented in Appendix D.5, where RAP-GNN also outperforms end-to-end.

**Large-Scale Graph Node Classification.** To further demonstrate the applicability of RAP-GNN, we now evaluate its performance on a node classification task using the large-scale ogbn-proteins and ogbn-products [Hu *et al.*, 2020] datasets. The results presented in Table 4 (using GCN) indicate that RAP-GNN delivers results on par with end-to-end training, while other baselines that employ random weights show a decline in performance, especially Random Weights and Fixed Random Weights on the ogbn-products dataset. A similar observation is made with GraphSage (Table 8 in Appendix D.3). These results underscore the effectiveness of RAP-GNN in achieving competitive performance and its versatility across different GNN backbones.

## 4.2 (A2) The Importance of On-The-Fly Sampling and Diagonal Weights

In this section, we study the design of RAP-GNN by examining its two key components: on-the-fly sampling and diagonal structured weights. First, we evaluate the significance of on-the-fly sampling by comparing RAP-GNN to Fixed Random Diagonal. Next, we explore the impact of the diagonal structure of  $\mathbf{w}^{(l)}$  by contrasting RAP-GNN with two addi-

tional baselines: Random Weights, which replaces diagonal weights in Equation (1) with full random matrices and sampling them on-the-fly, and Fixed Random Weights, which also employs full random matrices but keeps them fixed during the training phase instead of sampling them on-the-fly.

**The Importance of on-the-fly Sampling.** The results in Tables 1, 3 and 4 indicate that Fixed Random Diagonal performs comparably to RAP-GNN, though RAP-GNN consistently achieves slightly better results across all evaluated datasets for node tasks. Furthermore, on graph classification datasets, as shown in Table 2, RAP-GNN consistently outperforms Fixed Random Diagonal. These findings are especially noteworthy given that RC methods share similarities with the fixed random weights approach used in Fixed Random Diagonal, highlighting the advantage of on-the-fly sampling in delivering meaningful improvements over the fixed weight scheme.

**The Importance of Diagonal Weights.** All the results in Tables 1 to 4 show that the diagonal structure of  $\mathbf{w}^{(l)}$  is beneficial for downstream performance. Namely, RAP-GNN consistently outperforms the variants using a full random matrix among different graph tasks in all datasets, whether coupled with on-the-fly sampling (Random Weights) or fixed weights (Fixed Random Weights). Specifically, both Random Weights and Fixed Random Weights exhibit a notable performance gap compared to both end-to-end and RAP-GNN. Moreover, using full-weight matrices achieves lower or similar performance of Pretrained Embedding. The experimental results in Figure 2(c) underscore the significance of using diagonal weights and validate the findings of Observation 2. They show that both RAP-GNN and Fixed Random Diagonal, which incorporate diagonal random weights, sustain stable performance even as architectures deepen. In contrast, Random Weights and Fixed Random Weights, using full random weights, experience a sharp performance decline as more layers are added, with Random Weights exhibiting a rapid performance drop as more layers are added.

## 4.3 (A3) Memory and Time Consumption

In previous experiments, we have shown that RAP-GNN achieves accuracy comparable to end-to-end networks. Here, we shift the focus to empirically measure its efficiency. All the measurements discussed below are conducted on the PubMed dataset (19,717 nodes, 88,648 edges) using an NVIDIA GeForce RTX 4090 GPU.

**Runtimes.** We measure the average runtime per epoch during training and inference, using networks with varying numbers of GNN layers, from 2 to 32, with 256 hidden channels. Figure 2 shows the significant runtime efficiency of RAP-GNN compared to end-to-end training on both training and inference. As the number of GNN layers increases, the efficiency gap between RAP-GNN and end-to-end becomes more pronounced. For example, with 32 layers, RAP-GNN reduces training time by approximately 48ms, offering a 6× speedup. With 8 layers, RAP-GNN shows a reduction of 12ms, a 3× speedup, highlighting its scalability and efficiency. Although Fixed Random Diagonal and Fixed Random Weights also reduce training time by avoiding the

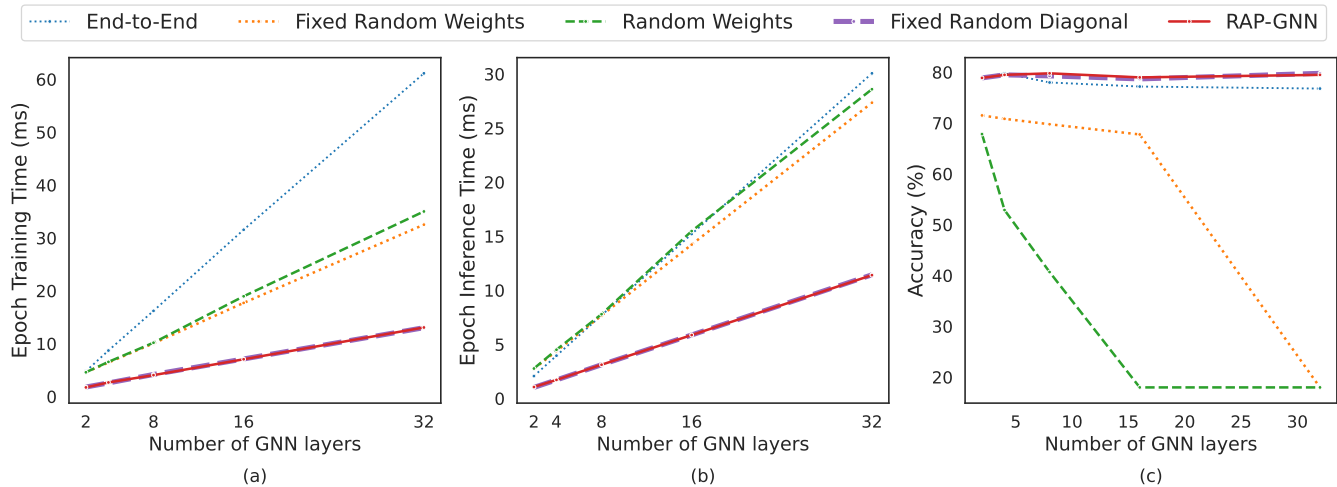


Figure 2: Training time (a), inference time (b), and accuracy (c) for node classification on PubMed with GCN backbone. The runtimes gap between our RAP-GNN and End-to-End widens as the number of layers increases, while obtaining superior accuracy than End-to-End. Accuracy results in (c) validate Observation 2, showing RAP-GNN maintains stability in deep architectures, unlike Random Weights.

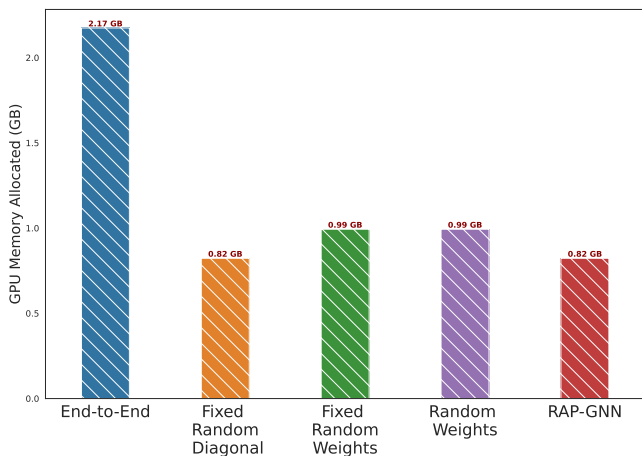


Figure 3: GPU memory usage comparison on the PubMed dataset: RAP-GNN requiring only a third of the memory compared to the End-to-End (GCN backbone).

need to train GNN layers and embedding layer, they remain slower than RAP-GNN and Fixed Random Diagonal. This is because RAP-GNN and Fixed Random Diagonal leverage diagonal weights during both training and evaluation, significantly reducing computations time.

**GPU Memory Consumption.** Additionally, we measure the memory consumption of RAP-GNN and end-to-end. To ensure a fair comparison, all networks are configured with 256 hidden dimensions and 32 layers. In Figure 3, the results highlight the resource efficiency of RAP-GNN. Although Random Weights and Fixed Random Weights show a reduction in GPU memory consumption compared to end-to-end, the decrease is more pronounced with RAP-GNN and Fixed Random Diagonal. Both RAP-GNN and Fixed Random Diagonal use one-third the memory used by end-to-

end. As noted in Section 3, two key factors contribute to these gains. First, the design of RAP-GNN eliminates the need for full backpropagation through the network, requiring gradient storage only for the final classifier layer. Second, the use of a diagonal matrix for  $\mathbf{w}^{(l)}$  allows matrix multiplication to be replaced with element-wise vector multiplication, reducing the number of parameters and floating-point operations.

A similar trend of reduced training and evaluation time, along with lower GPU memory consumption, is observed for the large-scale datasets ogbn-products and ogbn-proteins in Appendix D.3. Combined with the performance effectiveness presented in Section 4.1, these findings further highlight the applicability of RAP-GNN for real-world applications, where efficient processing of large graphs is essential.

## 5 Conclusion

In this work, we present Random Propagation Graph Neural Networks (RAP-GNN), offering an alternative to traditional end-to-end training in GNNs by replacing learnable weights in message-passing layers with diagonal random weight matrices sampled on-the-fly. RAP-GNN reduces training time by up to 6 $\times$  and memory usage by up to 3 $\times$ , while maintaining competitive accuracy across diverse graph tasks and datasets. In addition, we show that our design choices allow RAP-GNN to mitigate feature collapse and maintain feature diversity, addressing challenges faced by deep GNN architectures. Our experiments demonstrate the scalability and efficiency of RAP-GNN, particularly on large-scale datasets, where it achieves strong predictive performance with significantly lower computational overhead compared to fully trained counterparts. This research advances the research frontier of resource-efficient graph learning and lays the groundwork for future exploration of scalable, lightweight GNN architectures for practical applications.

## References

- Ralph Abboud, İsmail İlkan Ceylan, Martin Grohe, and Thomas Lukasiewicz. The surprising power of graph neural networks with random node initialization. In *International Joint Conference on Artificial Intelligence*, 2021.
- Pedro HC Avelar, Anderson R Tavares, Marco Gori, and Luis C Lamb. Discrete and continuous deep residual learning over graphs. *arXiv preprint arXiv:1911.09554*, 2019.
- Filippo Maria Bianchi, Claudio Gallicchio, and Alessio Micheli. Pyramidal reservoir graph neural network. *Neurocomputing*, 470, 2022.
- Lukas Biewald. Experiment tracking with weights and biases, 2020. Software available from wandb.com.
- Michael M Bronstein, Joan Bruna, Taco Cohen, and Petar Veličković. Geometric deep learning: Grids, groups, graphs, geodesics, and gauges. *arXiv preprint arXiv:2104.13478*, 2021.
- Tianlong Chen, Yongduo Sui, Xuxi Chen, Aston Zhang, and Zhangyang Wang. A unified lottery ticket hypothesis for graph neural networks. In *International Conference on Machine Learning*, 2021.
- Daiki Chijiwa, Shin’ya Yamaguchi, Yasutoshi Ida, Kenji Umakoshi, and Tomohiro Inoue. Pruning randomly initialized neural networks with iterative randomization. *Advances in neural information processing systems*, 34, 2021.
- Giovanni Donghi, Luca Pasa, Luca Oneto, Claudio Gallicchio, Alessio Micheli, Davide Anguita, Alessandro Sperduti, and Nicolò Navarin. Investigating over-parameterized randomized graph networks. *Neurocomputing*, 606, 2024.
- Vijay Prakash Dwivedi, Chaitanya K Joshi, Anh Tuan Luu, Thomas Laurent, Yoshua Bengio, and Xavier Bresson. Benchmarking graph neural networks. *Journal of Machine Learning Research*, 24, 2023.
- Moshe Eliasof, Fabrizio Frasca, Beatrice Bevilacqua, Eran Treister, Gal Chechik, and Haggai Maron. Graph positional encoding via random feature propagation. In *International Conference on Machine Learning*, 2023.
- Moshe Eliasof, Lars Ruthotto, and Eran Treister. Improving graph neural networks with learnable propagation operators. In *International Conference on Machine Learning*, 2023.
- Moshe Eliasof, Beatrice Bevilacqua, Carola-Bibiane Schönlieb, and Haggai Maron. Granola: Adaptive normalization for graph neural networks. *arXiv preprint arXiv:2404.13344*, 2024.
- Wenzheng Feng, Jie Zhang, Yuxiao Dong, Yu Han, Huanbo Luan, Qian Xu, Qiang Yang, Evgeny Kharlamov, and Jie Tang. Graph random neural networks for semi-supervised learning on graphs. *Advances in neural information processing systems*, 33, 2020.
- Matthias Fey and Jan Eric Lenssen. Fast graph representation learning with pytorch geometric. *arXiv preprint arXiv:1903.02428*, 2019.
- Claudio Gallicchio and Alessio Micheli. Graph echo state networks. In *International Joint Conference on Neural Networks*, 2010.
- Claudio Gallicchio and Alessio Micheli. Fast and deep graph neural networks. *AAAI Conference*, 2020.
- Thales Gonçalves and Luis Gustavo Nonato. Extreme learning machine to graph convolutional networks. In *Brazilian Conference on Intelligent Systems*, 2022.
- William L Hamilton, Rex Ying, and Jure Leskovec. Inductive representation learning on large graphs. In *Advances in neural information processing systems*, 2017.
- Weihua Hu, Matthias Fey, Marinka Zitnik, Yuxiao Dong, Michael Willatt, Bowen Liu, Michele Catasta, and Jure Leskovec. Open graph benchmark: Datasets for machine learning on graphs. *arXiv preprint arXiv:2005.00687*, 2020.
- Guang-Bin Huang, Qin-Yu Zhu, and Chee-Kheong Siew. Extreme learning machine: theory and applications. *Neurocomputing*, 70, 2006.
- Longteng Huang, Chao Zhang, Liang Tan, Dezhong Wang, Xuan Wang, Haifeng Liu, and Edward Y. Chang. Are powerful graph neural nets necessary? a dissection of graph classifiers. *arXiv preprint arXiv:2202.10471*, 2022.
- Tianjin Huang, Tianlong Chen, Meng Fang, Vlado Menkovski, Jiaxu Zhao, Lu Yin, Yulong Pei, Decebal Constantin Mocanu, Zhangyang Wang, Mykola Pechenizkiy, et al. You can have better graph neural networks by not training weights at all: Finding untrained gnns tickets. *arXiv preprint arXiv:2211.15335*, 2022.
- Herbert Jaeger. The “echo state” approach to analysing and training recurrent neural networks-with an erratum note. *German National Research Center for Information Technology*, 148, 2001.
- Thomas N Kipf and Max Welling. Semi-supervised classification with graph convolutional networks. *arXiv preprint arXiv:1609.02907*, 2016.
- Yuankai Luo, Lei Shi, and Xiao-Ming Wu. Classic gnns are strong baselines: Reassessing gnns for node classification. *arXiv preprint arXiv:2406.08993*, 2024.
- Andrew Kachites McCallum, Kamal Nigam, Jason Rennie, and Kristie Seymore. Automating the construction of internet portals with machine learning. *Information Retrieval*, 3, 2000.
- Christopher Morris, Martin Ritzert, Matthias Fey, William L Hamilton, Jan Eric Lenssen, Gaurav Rattan, and Martin Grohe. Tudataset: A collection of benchmark datasets for learning with graphs. *arXiv preprint arXiv:2007.08663*, 2020.
- Ryan Murphy, Balasubramaniam Srinivasan, Vinayak Rao, and Bruno Ribeiro. Relational pooling for graph representations. In *International Conference on Machine Learning*, 2019.

- Galileo Namata, Ben London, Lise Getoor, Bert Huang, and U Edu. Query-driven active surveying for collective classification. In *10th international workshop on mining and learning with graphs*, volume 8, 2012.
- Nicolò Navarin, Luca Pasa, Claudio Gallicchio, and Alessandro Sperduti. An untrained neural model for fast and accurate graph classification. In *International Conference on Artificial Neural Networks*, 2023.
- Luca Pasa, Nicolò Navarin, and Alessandro Sperduti. Multiresolution reservoir graph neural network. *IEEE Transactions on Neural Networks and Learning Systems*, 2021.
- Adam Paszke, Sam Gross, Francisco Massa, Adam Lerer, James Bradbury, Gregory Chanan, Trevor Killeen, Zeming Lin, Natalia Gimelshein, Luca Antiga, et al. Pytorch: An imperative style, high-performance deep learning library. *Advances in neural information processing systems*, 2019.
- Omri Puny, Heli Ben-Hamu, and Yaron Lipman. Global attention improves graph networks generalization. *arXiv preprint arXiv:2006.07846*, 2020.
- Vivek Ramanujan, Mitchell Wortsman, Aniruddha Kembhavi, Ali Farhadi, and Mohammad Rastegari. What’s hidden in a randomly weighted neural network? In *Proceedings of the IEEE/CVF conference on computer vision and pattern recognition*, 2020.
- Andreas Roth and Thomas Liebig. Rank collapse causes over-smoothing and over-correlation in graph neural networks. In *Learning on Graphs Conference*, pages 35–1. PMLR, 2024.
- Ryoma Sato, Makoto Yamada, and Hisashi Kashima. Random features strengthen graph neural networks. In *Proceedings of the SIAM SDM conference*, 2021.
- Prithviraj Sen, Galileo Namata, Mustafa Bilgic, Lise Getoor, Brian Galligher, and Tina Eliassi-Rad. Collective classification in network data. *AI magazine*, 29, 2008.
- Minjie Wang, Da Zheng, Zihao Ye, Quan Gan, Mufei Li, Xiang Song, Jinjing Zhou, Chao Ma, Lingfan Yu, Yu Gai, Tianjun Xiao, Tong He, George Karypis, Jinyang Li, and Zheng Zhang. Deep graph library: A graph-centric, highly-performant package for graph neural networks. *arXiv preprint arXiv:1909.01315*, 2019.
- Kun Wang, Yuxuan Liang, Pengkun Wang, Xu Wang, Pengfei Gu, Junfeng Fang, and Yang Wang. Searching lottery tickets in graph neural networks: A dual perspective. In *International Conference on Learning Representations*, 2023.
- Keyulu Xu, Weihua Hu, Jure Leskovec, and Stefanie Jegelka. How powerful are graph neural networks? In *International Conference on Learning Representations*, 2019.
- Junliang Yu, Hongzhi Yin, Xin Xia, Tong Chen, Lizhen Cui, and Quoc Viet Hung Nguyen. Are graph augmentations necessary? simple graph contrastive learning for recommendation. In *45th international ACM SIGIR*, 2022.
- Zijia Zhang, Yaoming Cai, Wenyin Gong, Xiaobo Liu, and Zhihua Cai. Graph convolutional extreme learning machine. In *International Joint Conference on Neural Networks*, 2020.
- Zijia Zhang, Yaoming Cai, and Wenyin Gong. Semi-supervised learning with graph convolutional extreme learning machines. *Expert Systems with Applications*, 213, 2023.

## A Additional Details

In this section, we begin by exploring how weights are typically utilized in common GNN backbones.

We first present GNN backbones with  $\mathbf{w}^{(l)}$  and later show how they are random sampled on-the-fly. In our experiments, we use two popular backbones: GCN [Kipf and Welling, 2016] with residual connections, and GIN [Xu *et al.*, 2019], defined as follows:

*GCN.* The forward pass for the  $l$ -th GCN layer with a residual connection, where  $\sigma(\cdot)$  is a non-linear activation function (ReLU), is given by:

$$\mathbf{h}^{(l)} = \mathbf{h}^{(l-1)} + \sigma\left(\tilde{\mathbf{A}}\mathbf{h}^{(l-1)}\mathbf{w}^{(l)}\right), \quad (2)$$

where  $\tilde{\mathbf{A}} = \mathbf{D}^{-\frac{1}{2}}\mathbf{A}\mathbf{D}^{-\frac{1}{2}}$ , where  $\mathbf{D}$  is the node degree-matrix.

*GIN.* The forward pass for the  $l$ -th GIN layer (with  $\epsilon = 0$ ) reads:

$$\mathbf{h}_v^{(l)} = \sigma\left(\mathbf{w}^{(l)}\left(\mathbf{h}_v^{(l-1)} + \sum_{u \in \mathcal{N}(v)} \mathbf{h}_u^{(l-1)}\right)\right) \quad (3)$$

where  $\mathbf{h}_v^{(l)}$  is the embedding of node  $v$  at the  $l$ -th layer,  $\mathcal{N}(v)$  denotes the set of neighbors of node  $v$ , and  $\sigma(\cdot)$  is a non-linear activation function (ReLU). Notably,  $\mathbf{w}^{(l)}$  can be extended to multiple weights  $\mathbf{w}_j^{(l)}$  for GIN.

In RAP-GNN, first we pretrain the node embedding  $f_\phi^{\text{pre}}$  as shown in Algorithm 1. During the main training phase, RAP-GNN samples  $L$  random vectors  $\alpha^{(l)} \in [0, 1]^d$  ( $l = 1, \dots, L$ ) and generates diagonal random GNN weight matrices  $\mathbf{w}^{(l)}$  with  $\alpha^{(l)}$ . Then RAP-GNN uses these weights in the corresponding GNN layers (Equations (2) and (3)) to obtain the final representations and trains  $c_\theta$  on the downstream task. The pseudo-code for the training phase is provided in Algorithm 2.

## B Additional Related Work

**Random Strategies to perform Graph Data Augmentations.** GRAND [Feng *et al.*, 2020] enhances the robustness of GNNs by randomly dropping node features, either partially (via dropout) or entirely, making each node stochastically pass messages to its neighbors. This strategy increases robustness by making nodes less sensitive to specific neighborhoods and decouples feature propagation from transformation, enabling higher-order propagation without added complexity or over-smoothing. While GRAND improves performance in semi-supervised graph tasks by generating diverse augmented representations, it still requires learning all network parameters. In contrast, our method achieves enhanced performance by leveraging random propagation for message passing, completely bypassing end-to-end training.

**Randomness in Recommendation Systems.** A new line of research explores incorporating randomness into graph-based recommendation systems to enhance contrastive learning as well as more computational efficiency. For example, Yu *et al.* [2022] propose adding noise directly to embeddings as an alternative to traditional graph augmentations in contrastive

---

### Algorithm 1 Pretraining $f_\phi^{\text{pre}}$ .

---

- 1: Initialize learning rate  $\eta^{\text{pre}}$  and maximal number of epochs MaxPreEpochs for the pretraining process.
  - 2: **for**  $i = 1$  to MaxPreEpochs **do**
  - 3:     **for**  $\mathbf{x}$  in Data **do**
  - 4:          $\hat{y} = c_{\phi'}^{\text{pre}} \circ f_\phi^{\text{pre}}(\mathbf{x})$
  - 5:         Compute the downstream task loss between the ground-truth  $y$  and  $\hat{y}$ .
  - 6:         Update  $c_{\phi'}^{\text{pre}}$  and  $f_\phi^{\text{pre}}$  parameters using a gradient-descent method (Adam) with a learning rate  $\eta^{\text{pre}}$ .
  - 7:     **end for**
  - 8: **end for**
- 

---

### Algorithm 2 Training $c_\theta$ .

---

- 1: Initialize learning rate  $\eta$  and max epochs MaxEpochs for the training process.
  - 2: **for**  $i = 1$  to MaxEpochs **do**
  - 3:     **for**  $\mathbf{x}$  in Data **do**
  - 4:         Sample  $L$  random vectors  $\alpha^{(l)} \in [0, 1]^d$   $\triangleright$
  - 5:          $l = 1, \dots, L$
  - 6:         Generate diagonal random GNN weight matrices  $\mathbf{w}^{(l)}$  with  $\alpha^{(l)}$   $\triangleright$  Equation (1)
  - 7:         Compute model output  $\hat{y} = f(\mathbf{x}, \mathbf{A})$
  - 8:         Update parameters  $\theta$  in classifier  $c_\theta$  using a gradient-descent method (Adam) with learning rate  $\eta$ .
  - 9:     **end for**
  - 10: **end for**
- 

learning, introducing randomness into representation learning. In contrast, RAP-GNN employs randomness in message propagation to boost performance.

**Graph Lottery-Ticket Hypothesis.** The Graph Lottery-Ticket hypothesis, introduced in recent years [Chen *et al.*, 2021; Wang *et al.*, 2023], suggests that it is possible to identify sparse sub-networks that perform as well as end-to-end trained models. However, this approach requires pretraining the entire network to discover these sub-networks, which remains computationally intensive. Recent work expands this idea by identifying sub-networks within randomly weighted networks. Ramanujan *et al.* [2020] apply this to vision tasks, showing that pruning can match the performance of end-to-end optimized networks. Nevertheless, their method demands over-parameterized networks before pruning, increasing memory and computational requirements. Chijiwa *et al.* [2021] address this by re-randomizing weights during subsequent pruning iterations, reducing over-parameterization. More recently, Huang *et al.* [2022b] adapted pruning mask optimization for graph tasks. Unlike these methods, which focus on identifying efficient sub-networks without modifying weight values from randomly initialized networks, our approach seeks to match or surpass the competitive performance of end-to-end trained models by random propagation.

## C Rank Collapse

Observation 2 shows that RAP-GNN mitigates feature collapse especially when compared to GNNs with full random

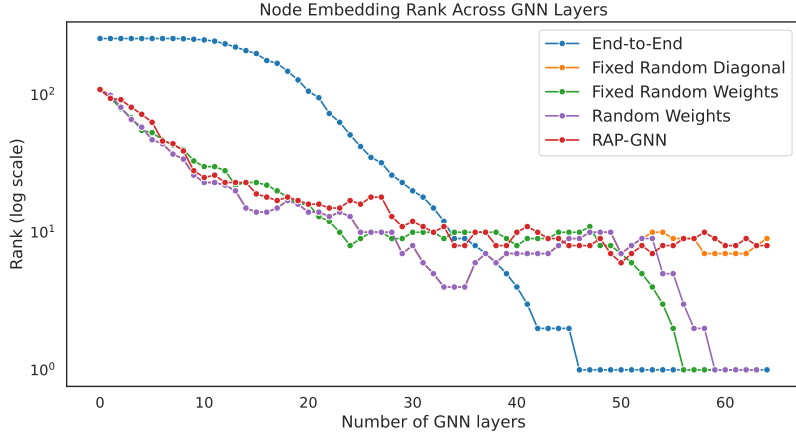


Figure 4: Comparison of the mean of  $\text{Var}(\mathbf{h}^{(l)})$  (in log scale) across layers for End-to-End and RAP-GNN on the PubMed dataset using the same GCN architecture with residual connections with  $L = 64$  and  $d = 256$ . RAP-GNN increases embedding variance with higher rate compared to End-to-End as the number of layers grows, consistent with the theoretical result in Observation 2.

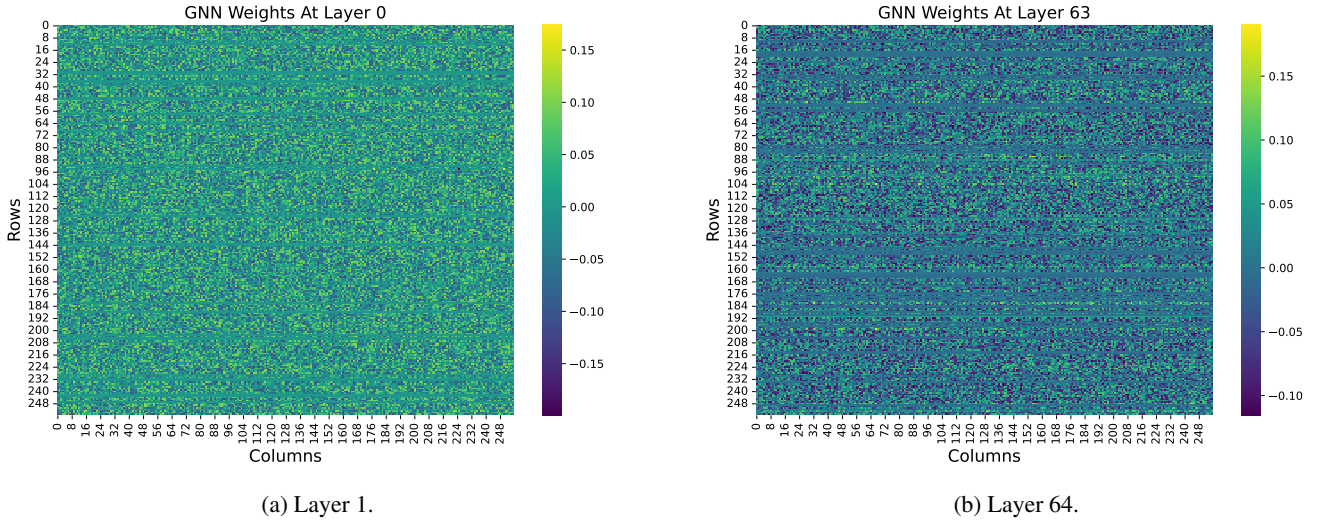


Figure 5: Weight matrices learned in an end-to-end trained GCN with residual connections are shown for layer 1 (a) and layer 64 (b), each sized  $256 \times 256$ . Notably, the learned matrices are not diagonal.

weights of the same depth, we also observe that *in practice* RAP-GNN exhibits significantly higher rank, and therefore less feature collapse, than GNNs with learnable weights.

These findings align closely with our experimental observations, as shown in Figure 4, which compares the rank  $\text{rank}(\mathbf{h}^{(l)})$  across layers for an end-to-end trained GCN, Fixed Random Diagonal, Fixed Random Weights, Random Weights, and RAP-GNN. Both RAP-GNN and Fixed Random Diagonal, which use diagonal weights, exhibit only a slight decrease in the rank of the embedding, in line with Observation 2, effectively preventing the feature collapse phenomenon. In contrast, models using full random weights, including End-to-End, Random Weights, and Fixed Random Weights, experience a sharp decline in  $\text{rank}(\mathbf{h}^{(l)})$  to 1, signaling a feature collapse. In addition, we note that, while in end-to-end trained GNNs, the weight matrices,  $\mathbf{w}^{(l)}$ , could

be learned to be diagonal, we do not observe this behavior in practice. Specifically, we illustrate the learned  $\mathbf{w}^{(l)}$  at layer 1 and layer 64 for an end-to-end trained GCN (Figure 5). In both cases, the learned weight matrices are not diagonal. The results in Figure 4 and Figure 5 were conducted on the PubMed dataset using the same GCN architecture with 64 layers ( $L = 64$ ) with residual connections.

Moreover, as shown in Figure 2(c), our RAP-GNN, and Fixed Random Diagonal consistently maintain stable performance as the number of layers increases, effectively mitigating the challenges posed by feature collapse. In contrast, GNNs with full random weights (Random Weights, Fixed Random Weights, and End-to-End) experience a significant decline in performance with increasing depth due to the loss of embedding diversity.

The consistency between the theoretical understanding in

Method ↓ / Dataset →	CORA	CITeseer	PUBMED
End-to-End	81.50 ± 4.8	71.10 ± 0.7	79.00 ± 0.6
Identity Weights	80.36 ± 0.4	69.32 ± 0.2	78.91 ± 0.3
Fixed Random Diagonal	81.32 ± 0.8	70.12 ± 0.9	78.00 ± 0.9
Fixed Random Weights	58.70 ± 1.8	55.88 ± 1.2	71.52 ± 0.6
Random Weights	23.29 ± 9.2	45.85 ± 7.7	67.85 ± 1.7
RAP-GNN (Ours)	82.42 ± 0.3	70.75 ± 0.3	78.94 ± 0.4

Table 5: Node classification accuracy comparison (%) $\uparrow$  of RAP-GNN, End-to-End, and other baselines using random weights. The results demonstrate that RAP-GNN, employing on-the-fly diagonal random weights in GNN layers, consistently outperforms all baselines using random weights while achieving competitive accuracy and, in some cases, surpassing End-to-End.

Observations 1 and 2 and the empirical results underscores the ability of RAP-GNN to preserve diversity in embeddings, also in deep architectures.

## D Additional Experiments

In this section, we present additional results to further analyze the performance of RAP-GNN.

First, in Appendix D.1, we expand on the results of Section 4.2 by comparing to an additional baseline of RAP-GNN. In Appendix D.2, we study the impact of pretraining the initial embedding. In Appendix D.3, we provide results for RAP-GNN on the larger ogbn-proteins dataset, comparing its performance against end-to-end trained networks. Finally, we assess the performance of RAP-GNN across various batch sizes in Appendix D.4, demonstrating its adaptability for practical applications.

### D.1 Identity as an Additional Baseline

We consider an additional baseline of RAP-GNN:

- Identity Weights: All GNN layer weights,  $w^{(l)}$ , are set to identity matrices.

Table 5 presents the results for the various RAP-GNN baselines. Among them, Identity Weights shows the lowest performance, indicating that simply passing input representations unchanged, is insufficient to obtain performance comparable to end-to-end training. On the contrary, RAP-GNN outperforms all its baselines that also do not train the GNN weights, and is competitive to end-to-end, underscoring the effectiveness of on-the-fly randomly sampled diagonal matrices in RAP-GNN.

### D.2 The Importance of Pretraining the Initial Embedding

In this section, we examine the importance of pretraining the initial embedding on the performance. We explore five setups for the embedding layer: (i) the Identity Embedding (Identity Embedding), where the initial embedding corresponds to the identity matrix; (ii) Fixed Random Embedding (Fixed Random Embedding), which samples a random full-weight matrix initially and keeps it fixed, (iii) Random Embedding

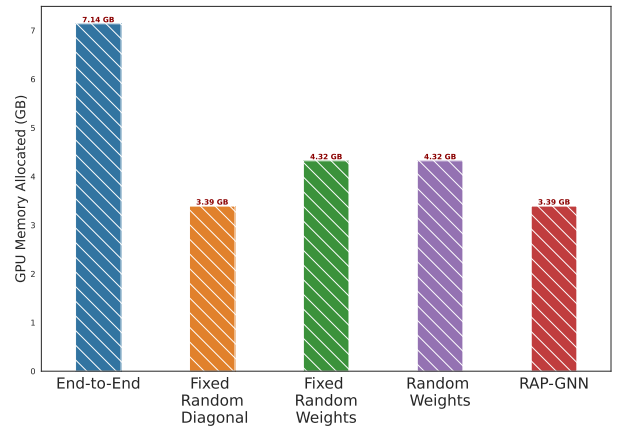


Figure 6: Comparison of GPU memory consumption on the ogbn-proteins dataset. Our RAP-GNN significantly reduces GPU memory consumption.

which samples a random full-weight matrix on-the-fly for every forward call (iv) Learnable Embedding, where the embedding layer weights are learned alongside the classifier, and lastly, (v) pretraining the embedding, as done in our RAP-GNN. All the embedding layers in this section are constructed as an MLP.

The results are presented in Table 6. Random Embedding setup struggles to learn across all datasets, indicating that randomization with on-the-fly sampling in both the initial embedding and the GNN layers hinders effective learning. Similarly, the Identity Embedding setup results in performance drops on Cora and PubMed and leads to Out-of-Memory (OOM) issues on CiteSeer, which has more features, underscoring the impracticality of this approach. Thus, we need an initial embedding to map  $c$  input features into a hidden dimension  $d$ , allowing all  $w^{(l)}$  to be diagonal matrices and preventing OOM issues. layers. Fixed Random Embedding shows good performance on Cora and CiteSeer but does not show significant gains on PubMed, and suffers from large variance. Learnable Embedding, which can be viewed as the upper bound for RAP-GNN, performs well across all datasets, even surpassing the end-to-end trained GCN. However, it requires backpropagation through the entire network despite only updating the embedding and classifier, impacting scalability. RAP-GNN offers a more balanced solution, achieving good performance while avoiding backpropagating through the GNN layers.

### D.3 Results on Large Scale Graphs

In addition to the accuracy results presented in Table 4, we further evaluate the performance of RAP-GNN on the ogbn-proteins and ogbn-products datasets, including running time and GPU memory consumption. All experiments were conducted on an NVIDIA RTX 4090.

**ogbn-proteins.** To evaluate the scalability of RAP-GNN, we conduct experiments on the large-scale ogbn-proteins dataset. We evaluate RAP-GNN and all baselines using a GCN backbone with residual connections. The pretrained embedding layer in RAP-GNN and its baselines that also

Method ↓ / Dataset →	CORA	CITeseer	PUBMED
End-to-End	81.50 ± 0.8	70.90 ± 0.7	79.00 ± 0.6
Identity Embedding + Random Diagonal	78.44 ± 3.0	OOM	73.46 ± 1.1
Fixed Random Embedding + Random Diagonal	82.82 ± 1.0	71.48 ± 0.7	78.76 ± 0.6
Random Embedding + Random Diagonal	26.30 ± 6.1	25.22 ± 0.9	37.28 ± 1.4
Learnable Embedding + Random Diagonal	84.36 ± 0.3	72.16 ± 0.6	79.32 ± 0.3
Pretrained Embedding + Random Diagonal (RAP-GNN)	82.42 ± 0.3	70.75 ± 0.3	78.94 ± 0.4

Table 6: Node classification accuracy (%)↑ using a GCN backbone with different embedding strategies. While Learnable embedding performs well across all datasets, it requires backpropagating through the random GNN layers despite only updating the embedding and the classifier. In contrast, using a Pretrained embedding as in RAP-GNN avoids backpropating through the GNN layers while achieving competitive performance.

Method ↓	OGBN-PROTEINS		
	ROC-AUC(%) ↑	Train time(ms) ↓	Eval. time(ms) ↓
Pretrained Embedding	71.07 ± 0.36	2,803	1,540
End-to-End	77.29 ± 0.46	14,078	9,969
Fixed Random Diagonal	76.84 ± 0.32	7,835	7,022
Fixed Random Weights	73.71 ± 0.71	9,545	9,920
Random Weights	70.46 ± 0.74	9,809	9,258
RAP-GNN (Ours)	77.01 ± 0.38	7,952	7,401

Table 7: Node classification ROC-AUC (%) along with training and evaluation times (ms) on the large ogbn-proteins dataset using a GCN [Kipf and Welling, 2016] backbone. RAP-GNN achieve comparable ROC-AUC with end-to-end training, as well as reduced runtimes.

sample random weights consists of exactly one single GNN layer. Further details on the implementation and hyperparameter search can be found in Appendix E.

As shown in Table 7, RAP-GNN achieves performance comparable to end-to-end while requiring significantly less time per epoch for both training and evaluation, as well as using less than half of the memory of an end-to-end GCN (Figure 6). Although Fixed Random Diagonal also achieves efficiency in time and GPU memory consumption, its performance is slightly lower than that of end-to-end and our RAP-GNN. On the other hand, Random Weights and Fixed Random Weights exhibit poor performance in both efficiency and efficacy.

**ogbn-products.** We further evaluate the performance of RAP-GNN on the ogbn-products dataset with the GraphSage backbone [Hamilton *et al.*, 2017], as well as the running time of RAP-GNN and all baselines. The results in Table 8 demonstrate that RAP-GNN offers a balanced approach between accuracy and computational efficiency when compared to End-to-End in both backbones. Specifically, we note that on both GCN and GraphSage backbones, our RAP-GNN achieves comparable accuracy to its corresponding end-to-end trained counterpart, while requiring significantly reduced training and evaluation times. In contrast, other baselines using random weights (Random Weights, Fixed Random Weights, and Fixed Random Diagonal) show a drop in performance, although they demonstrate gains in efficiency.

#### D.4 Effect of Batch Size on RAP-GNN Performance

Since each  $\mathbf{w}^{(l)}$  is sampled anew for every forward pass — remaining consistent across all graphs within the same batch

but varying between batches — it is important to evaluate the impact of batch size. To this end, we conducted additional experiments using the PROTEINS dataset. The results, summarized in Table 9, show that batch size has minimal influence on the performance of RAP-GNN. Specifically, RAP-GNN achieves consistent accuracy across varying batch sizes, with only minor variations observed. These findings demonstrate the robustness of RAP-GNN to different batch size settings, underscoring its flexibility in practical applications.

#### D.5 Results on ogbg-molbace

In addition to the results on the OGB datasets presented in Table 3, we now include results for the ogbg-molbace dataset in Table 10. Similar to the patterns observed in other datasets, RAP-GNN outperforms all evaluated baselines.

### E Dataset and Experiment Details

#### E.1 Dataset Statistics

In this section, we provide a summary of all the datasets used in this paper, as detailed in Table 11. The datasets contain a variety of types, graph tasks, and sizes, ensuring a fair comparison and comprehensive evaluation across experiments.

#### E.2 Experimental Details

Our experiments were conducted using the PyTorch [Paszke *et al.*, 2019] and PyTorch Geometric [Fey and Lenssen, 2019] frameworks, utilizing Weight and Biases [Biewald, 2020] for hyperparameter sweeps. In this section, we provide details on our specific implementation of the experiments.

Tables 12 to 14 outline the hyperparameter search space for all datasets divided by their collections. Specifically, Table 13

Backbone	Method	OGBN-PRODUCTS		
		Accuracy (%) $\uparrow$	Train time (ms) $\downarrow$	Eval. time (ms) $\downarrow$
GCN	Pretrained Embedding	72.83 $\pm$ 0.40	4,722	2,861
	End-to-End	75.90 $\pm$ 0.31	15,998	12,023
	Fixed Random Diagonal	74.93 $\pm$ 0.78	9,801	9,094
	Fixed Random Weights	27.72 $\pm$ 0.79	13,036	12,016
	Random Weights	26.08 $\pm$ 0.82	13,164	12,165
	RAP-GNN (Ours)	75.60 $\pm$ 0.88	9,861	9,124
GraphSage	Pretrained Embedding	74.72 $\pm$ 0.11	3,338	2,084
	End-to-End	78.29 $\pm$ 0.16	11,865	8,548
	Fixed Random Diagonal	76.28 $\pm$ 0.39	7,748	7,083
	Fixed Random Weights	27.03 $\pm$ 0.47	9,895	9,082
	Random Weights	26.90 $\pm$ 0.32	9,926	9,148
	RAP-GNN (Ours)	77.74 $\pm$ 0.43	7,934	7,109

Table 8: Performance Comparison on ogbn-products using GCN [Kipf and Welling, 2016] and GraphSage [Hamilton *et al.*, 2017] backbones. Accuracy (%), Training Time (ms), and Evaluation Time (ms) are reported.

Method	PROTEINS		
	Batchsize=256	Batchsize=512	Batchsize=1024
RAP-GNN (Ours)	75.1 $\pm$ 3.3	75.9 $\pm$ 3.8	75.0 $\pm$ 3.1

Table 9: Performance of RAP-GNN with varying batch sizes on TU-Dataset (PROTEINS) using GIN backbone [Xu *et al.*, 2019].

Method $\downarrow$	MOLBACE
	ROC-AUC $\uparrow$
Pretrained Embedding	65.64 $\pm$ 3.57
End-to-End	72.97 $\pm$ 4.00
Fixed Random Diagonal	72.68 $\pm$ 3.10
Fixed Random Weights	56.80 $\pm$ 5.55
Random Weights	55.23 $\pm$ 6.21
RAP-GNN (Ours)	73.42 $\pm$ 2.59

Table 10: Graph classification performance (%)  $\uparrow$  of RAP-GNN on the molbace dataset.

includes all datasets from the Planetoid collection, Table 14 presents datasets from the TUDatasets collection, and Table 12 outlines the OGB collection. Note that all  $\mathbf{w}^{(l)}$  matrices must be square, which requires the input and output dimensions of all hidden layers in  $g_{\mathbf{w}^{(l)}}$  to be the same, corresponding to the HIDDEN DIM. We use  $L$  to denote the number of hidden GNN layers. Square brackets  $[\ ]$  indicate ranges, and curly braces  $\{ \}$  represent sets for all tables.

**Node Classification Tasks.** For the Cora, CiteSeer, and PubMed datasets, all networks use a GCN backbone. The end-to-end trained networks implementation follows the PyTorch Geometric example, incorporating residual connections [Avelar *et al.*, 2019]. All baselines of RAP-GNN use MLP-based embeddings as the initial node embeddings. The number of MLP layers for the embedding is treated as a hyperparameter, while the hidden and output dimensions of the MLP are equal to  $d$ . All hyperparameter search details are in Table 13.

For the ogbn-proteins dataset, the implementation is based on Luo *et al.* [2024] with a GCN backbone. The embedding is a single GCN layer. The evaluation metric for the ogbn-proteins dataset follows Hu *et al.* [2020] and uses the ROC-AUC for binary classification. Details of all hyperparameters are given in Table 12.

For the ogbn-products dataset, we construct RAP-GNN using the implementation of a GCN or GraphSage backbone provided by Wang *et al.* [2019]. The embedding consists of a single GCN or GraphSage layer, matching the GNN layers used in the model. The evaluation metric for this dataset aligns with the multi-class classification approach outlined in Hu *et al.* [2020]. Detailed hyperparameter settings are provided in Table 12.

In all node classification tasks, batching is not required for either training or evaluation; therefore, the batch size rows in Tables 12 and 13 are left blank. For all considered experiments in all node classification tasks, we show the mean  $\pm$  std. of 5 runs with different random seeds.

**Graph Classification Tasks.** For the TUDatasets, we use the GIN baseline (employing 1-hidden-layer MLP inside) implementation from the PyTorch Geometric example. All baselines of RAP-GNN use MLP-based initial node embeddings, with the number of layers treated as a hyperparameter, and hidden and output dimensions of the MLP equal to  $d$ . Additionally, we follow the procedure in Xu *et al.* [2019], namely, we perform 10-fold cross-validation and report the validation mean and standard deviation at the epoch that achieved the maximum averaged validation accuracy. Details of all hyperparameters are provided in Table 14.

For the OGB datasets, we adopt the GIN network for training and evaluation, following the example code from Hu *et al.* [2020]. The embedding  $f_{\phi}^{\text{pre}}$  is identical to all other GNN layers, incorporating a 2-hidden-layer MLP with hidden and output dimensions equal to  $d$  within each GIN layer. The four datasets used for evaluation are molesol, moltox21, molbace, and molhiv from Hu *et al.* [2020]. Furthermore, for all considered experiments under node classification using OGB datasets, we show the mean  $\pm$  std. of 5 runs with different

	Dataset	Task	#Graphs	Avg. #Nodes	Avg. #Edges	#Classes
<b>Planetoid</b>	CORA	N	1	2,708	10,556	7
	CITeseer	N	1	3,327	9,104	6
	PUBMED	N	1	19,717	88,648	3
<b>TU Datasets</b>	MUTAG	G	188	17.9	19.7	2
	PTC	G	344	14.29	14.69	2
	PROTEINS	G	1,113	39.1	72.8	2
<b>OGB</b>	MOLESOL	G	1,128	13.3	13.7	-
	MOLTOX21	G	7,831	18.6	19.3	-
	MOLHIV	G	41,127	25.5	27.5	2
	MOLBACE	G	1,513	34.1	36.9	2
	OGBN-PROTEINS	N	1	132,534	39,561,252	112
	OGBN-PRODUCTS	N	1	2,449,029	61,859,140	47

Table 11: Overview of the graph learning datasets. N denotes a Node-level task, and G denotes a Graph-level task.

Hyperparameter	MOLESOL	MOLTOX21	MOLHIV	MOLBACE	OGBN-PROTEINS	OGBN-PRODUCTS
#LAYER in $f_\phi^{\text{pre}}$	1	1	1	1	1	1
#LAYER in $c_\theta$	1	1	1	1	{2, 3, 4}	1
L	{1, 2, 3}	{2, 3, 4}	{1, 2, 4, 6, 8}	{2, 4, 6}	{3, 4, 6, 8}	{2, 3, 4}
LR	[0.001, 0.05]	[0.005, 0.01]	[0.001, 0.05]	[0.0005, 0.01]	[0.007, 0.1]	[0.003, 0.03]
HIDDEN DIM.	{16, 32}	{8, 16}	{32, 64, 128, 256}	{32, 64, 128}	{240, 360}	{256, 300}
#EPOCHS	350	{350, 500}	{350, 500, 1000}	350	{500, 1000}	{20, 30}
BATCH SIZE	{256, 512}	512	-	512	-	-
DROPOUT	[0, 0.6]	[0, 0.5]	[0, 0.5, 0.6]	[0.4, 0.6]	[0.2, 0.6]	[0.15, 0.3]

Table 12: Hyperparameter search for the datasets in the OGB collection: molesol, moltox21, molhiv, molbace, ogbn-proteins, and ogbn-products.

Hyperparameter	CORA	CITeseer	PUBMED
#LAYER in $f_\phi^{\text{pre}}$	{1, 2}	{1, 2, 3}	{1, 2, 3}
#LAYER in $c_\theta$	1	1	1
L	{2, 4, 8, 16}	{2, 4, 6}	{4, 6, 8, 12}
LR	[0.001, 0.01]	[0.001, 0.01]	[0.001, 0.01]
HIDDEN DIM.	{16, 32}	{16, 32, 64, 128}	{16, 64, 128, 256}
#EPOCHS	700	1000	1000
BATCH SIZE	-	-	-
DROPOUT	[0, 0.5]	[0, 0.5]	[0, 0.5]

Table 13: Hyperparameter search for the Planetoid datasets.

random seeds. More details of the hyperparameter search are in Table 12.

Hyperparameter	MUTAG	PTC	PROTEINS
#LAYER in $f_\phi^{\text{pre}}$	{1, 2, 3}	{1, 2, 3}	{1, 2, 3}
#LAYER in $c_\theta$	2	2	1
L	{1, 2, 3}	{2, 3, 4, 6}	{1, 2, 3, 4}
LR	[0.007, 0.05]	[0.007, 0.05]	[0.007, 0.05]
HIDDEN DIM.	{16, 64, 128}	{16, 64, 128}	{16, 32, 64}
#EPOCHS	1000	1000	1000
BATCH SIZE	{64, 128, 512}	{64, 128, 512}	{128, 256, 512}
DROPOUT	[0, 0.35]	[0, 0.35]	[0, 0.35]

Table 14: Hyperparameter search for the TUDatasets.